Vol. 568: 101–110, 2017
https://doi.org/10.3354/meps12059

MARINE ECOLOGY PROGRESS SERIES
Mar Ecol Prog Ser

Published March 24

Nematocyst distribution corresponds to prey capture location in hydromedusae with different predation modes

Marco Corrales-Ugalde[1,*], Sean P. Colin[2,3], Kelly R. Sutherland[1]

[1]Oregon Institute of Marine Biology, University of Oregon, Eugene, Oregon 97403, USA
[2]Department of Marine Biology and Environmental Science, Roger Williams University, Bristol, Rhode Island 02809, USA
[3]Whitman Center, Marine Biological Laboratory, Woods Hole, Massachusetts 02543, USA

ABSTRACT: Understanding the factors that control predation in pelagic communities can inform predictions of community structure in marine ecosystems. Ubiquitous and selective predators such as cnidarian hydromedusae rely on their nematocysts to capture and retain prey but it is not clear how the density and spatial distribution of these cells relate to predation mode. We examined the relationship between prey capture and nematocyst distribution in the tentacles of *Aglantha digitale* and *Proboscidactyla flavicirrata*, which are considered ambush predators, and *Clytia gregaria* and *Mitrocoma cellularia*, which are considered feeding-current predators. First, we analyzed video of predator–prey interactions to compare capture locations of *Artemia* nauplii relative to the bell margin of each species. Second, tentacles of the same 4 species plus *Sarsia tubulosa* and *Aequorea victoria* were analyzed using microscopy to determine nematocyst distribution along their lengths. By analyzing behavior and morphology simultaneously, we found that the ambush predators *A. digitale* and *P. flavicirrata* have higher nematocyst density far from the bell and tend to capture more prey in the same region. In contrast, the feeding-current predators *C. gregaria* and *M. cellularia* capture most of their prey close to the bell, where they also show a slight increase in nematocyst densities. The presence of high nematocyst densities in regions where prey are likely to contact feeding structures serves to increase capture efficiencies. Quantifying the relationship between prey capture and nematocyst locations for different foraging strategies will strengthen the ability of researchers to predict feeding behavior based on morphological features.

KEY WORDS: Feeding behavior · Functional morphology · Predation · Zooplankton · *Aequorea victoria* · *Aglantha digitale* · *Clytia gregaria* · *Mitrocoma cellularia* · *Proboscidactyla flavicirrata* · *Sarsia tubulosa*

INTRODUCTION

Cnidarian medusae are significant and sometimes dominant predators in coastal and open ocean ecosystems and are capable of substantially reducing standing stocks of prey (Purcell et al. 1987, Purcell & Grover 1990). Their ecological role has the potential to become more pronounced in response to jellyfish population increases as marine ecosystems undergo environmental changes (Purcell 2005, Richardson 2008). Selective predation by cnidarians such as hydromedusae (Larson 1987, Purcell 1997) may ultimately determine the community structure of lower trophic levels (Brooks & Dodson 1965, Fields & Yen 1997). Prey selectivity is driven in part by specialized feeding mechanisms (Fields & Yen 1997), and in hydromedusae, feeding strategies are determined by body morphology and behavior (Mills 1981, Colin & Costello 2002, Colin et al. 2003, Dabiri et al. 2010). Thus, analyzing morphological factors related to pre-

*Corresponding author: mcugalde88@gmail.com

dation in hydromedusae can elucidate how different morphologies might be suited to specific prey types (Greene 1988, Regula et al. 2009).

One morphological feature, the fineness ratio (bell height/width), correlates with both swimming and foraging strategies (Costello & Colin 1995, Costello et al. 2008). In oblate (disc-shaped) medusae with low fineness ratios, the cycles of bell contraction and relaxation generate vortices for propulsion as well as for prey entrainment (Ford et al. 1997, Colin & Costello 2002, Katija et al. 2011, Gemmell et al. 2015). Medusae that feed and swim in this way are considered feeding-current predators. In prolate (bullet-shaped) medusae with higher fineness ratios, swimming and feeding are decoupled (Colin & Costello 2002). Prolate medusae feed by extending their tentacles while remaining stationary in the water column (Purcell 1981, Greene 1985) and rely on prey colliding with the tentacles; thus they are considered ambush predators (Madin 1988, Hansson & Kiørboe 2006, Regula et al. 2009).

In addition to swimming and foraging strategies, tentacle arrangement and spacing influence how medusae encounter prey (Madin 1988). For example, the scyphozoan feeding-current medusa *Chrysaora quinquecirrha* does not capture prey uniformly along the length of the tentacles; instead, most prey are captured at the proximal part of the tentacles, closer to the bell margin (Ford et al. 1997). Prey capture locations have not been studied in other cnidarian medusae, and we lack an understanding of how prey are captured along the tentacles of ambush-feeding medusae.

Once medusae encounter prey, nematocysts in the tentacles capture and retain the prey item. Previous morphological descriptions of hydromedusae have recognized different patterns of nematocyst distribution and density in the tentacles. For instance, nematocysts can be more concentrated to one side of the tentacle or at the tentacle tips, and can be either evenly distributed or arranged in clusters (Bouillon 1985, Purcell & Mills 1988). Nematocyst density is a relevant factor that can determine capture efficiency, since adherence force between the predator's tentacles and prey increases with the number of nematocysts fired (Thorington & Hessinger 1996). It is unclear, however, if the patterns of nematocyst distribution are related to prey capture locations and foraging strategy.

Nematocyst type also mediates prey selectivity. Medusae of the orders Trachylina and Anthoatecata, which feed on crustaceans, have nematocyst types that either penetrate or adhere to the prey surface, whereas Leptomedusae, which eat mostly soft-bodied prey such as gelatinous zooplankton and eggs, lack surface-adhering nematocysts (Purcell & Mills 1988). Adherence force between the predator and prey can change depending on the amount of each nematocyst type fired (Thorington & Hessinger 1996); thus the density of each nematocyst type is another determinant of prey selection.

Using a comparative approach, we analyzed the relationship between prey capture and nematocyst distribution in 6 species of coexisting hydromedusae with distinct morphologies and predatory modes: the prolate ambush predators *Aglantha digitale* (O.F. Müller, 1776), *Proboscidactyla flavicirrata* (Brandt, 1835) and *Sarsia tubulosa* (M. Sars, 1835), and the oblate feeding-current medusae *Clytia gregaria* (Agassiz, 1862), *Mitrocoma cellularia* (Agassiz, 1862) and *Aequorea victoria* (Murbach & Shearer, 1902). These species represent 3 orders: *A. digitale* and *P. flavicirrata* are Trachymedusae, *S. tubulosa* is an Anthomedusa and *C. gregaria*, *M. cellularia* and *A. victoria* are Leptomedusae. First, we used video observations to compare capture locations of *Artemia* nauplii relative to the bell margin in 4 species (*A. digitale*, *P. flavicirrata*, *C. gregaria*, *M. cellularia*). Then we analyzed tentacle images of all 6 species to determine whether nematocyst density and distribution varied among species with different morphologies and feeding modes.

MATERIALS AND METHODS

Specimen collection and handling

For the behavioral and morphological studies, we hand-collected specimens of the ambush predators *Aglantha digitale*, *Proboscidactyla flavicirrata* and *Sarsia tubulosa*, and the feeding-current predators *Aequorea victoria*, *Clytia gregaria* and *Mitrocoma cellularia* from surface waters off the dock at Friday Harbor Marine Laboratories, Washington, USA during June and July 2015. Organisms used for behavioral analyses were maintained, unfed, in an aquarium with running sea water for a period of 24 h before video recording commenced.

Analysis of prey capture locations

Videos for behavioral analyses were made using a Sony HD Digital Video Camcorder recording at 30 frames s^{-1}. Filming vessels (12.5 × 6.5 × 2.5 cm) were filled with sea water and contained a single hydro-

medusa plus hatched *Artemia* nauplii. *Artemia* nauplii are a useful prey type when the main goal is to analyze a predator's behavior, since nauplii are readily captured and ingested by the cnidarian predators in this study and do not exhibit strong escape responses (Ford et al. 1997, Colin et al. 2015). A collimated white LED light with a diffuser filter was placed behind the filming vessel and directed at the camera lens to create bright field illumination and enhance contrast of the predator and prey bodies. When the hydromedusa was small (<5 mm diameter), a 10× magnifying lens was placed in front of the camera lens to decrease the field of view. Since *A. digitale* consistently swam away from the filming area, these medusae were tethered to a capillary pipette using methods similar to Regula et al. (2009). Based on our observations, this procedure did not inhibit feeding behavior. Due to the larger size of *M. cellularia*, these observations were conducted in a 22.5 × 16.5 × 7.5 cm vessel. *Sarsia tubulosa* has very long tentacles and *A. victoria* has a large bell diameter compared to the other species, which precluded feeding behavior observations in these species.

Capture was defined as prey attaching to the tentacles for more than 1 s (Hansson & Kiørboe 2006), and measurements were limited to events within the focal plane. Prey capture locations were measured based on the distance from the bell margin (d) using ImageJ (National Institutes of Health). This distance was standardized by the equivalent spherical diameter (ESD) of each individual hydromedusa. ESD is defined as the diameter of a sphere with the same volume of an animal (Pitt et al. 2013), and for medusae the volume can be estimated as half the volume of a hemi-ellipsoid: $[(\frac{4}{3}\pi hr^2) \div 2]$, where h is the bell height and r is the bell radius. This standardization allowed for comparisons between medusae with different morphologies (Hirst et al. 2003, Pitt et al. 2013).

Nematocyst density and distribution in the tentacles

To measure nematocyst distribution, medusae were placed in a solution of $MgCl \cdot 6H_2O$ in fresh water (~5% m v^{-1}) for 5 min, and tentacles were removed from the umbrellar margin. Tentacle length was measured when relaxed, prior to dissection. Once dissected, the tentacle was placed on a glass slide and photographed from the base toward the tip using a Nikon E 600 microscope equipped with phase and differential interference optics. Tentacle bulbs were excluded from the analyses since nematogenesis occurs in this region (Denker et al. 2008). If the tentacle remained contracted or was torn, damaged, or stretched either during the dissection process or when placed between the slide and the cover slip, the sample was discarded. Multiple tentacles from the same individual were dissected in instances where there were limited specimens available. Images were collated using Adobe Photoshop CS5 and the full tentacle picture was divided into 10 equal sections, with 0% representing the tentacle base and 100% representing the full tentacle length. This method allowed for direct comparisons between tentacles of differing lengths. Using ImageJ, a minimum of 5000 μm^2 of the tentacle area was examined to obtain the number of nematocysts per 1000 μm^2, similar to Regula et al. (2009). Nematocyst types were identified according to the capsule sizes reported in Purcell & Mills (1988) and using the nomenclature established by Östman (2000). In some cases more than one tentacle was analyzed per individual; thus, the numbers of individuals analyzed per species are reported as 'N' and the tentacle sample sizes are reported as 'n'.

Morphological and behavioral data analysis

The standardized capture distance (d/ESD) and nematocyst density (nematocysts per 1000 μm^2) were averaged across individuals, and non-parametric Kruskal-Wallis (KW) tests were used to compare means of these variables in the species analyzed. We also performed KW tests to compare the means of each nematocyst type in *A. digitale*, *P. flavicirrata*, *S. tubulosa* and *A. victoria*. Data for each species were pooled across individuals, and weighted arithmetic means were reported since there were more observations from some individuals than others. If the differences among rank means were significant, post hoc comparisons between species were made with a Bonferroni-Dunn test. To assess the spatial distribution of nematocysts in each medusa species, linear regressions were performed to determine how nematocyst density changes along the tentacle length. Positive slopes indicated increasing nematocyst densities towards the tentacle tips, whereas negative slopes indicated decreasing nematocyst densities. All analyses were performed in RStudio 0.98.1091. KW and Bonferroni-Dunn tests were performed using the 'dunn.test' package (Dinno 2016) following Dunn (1961).

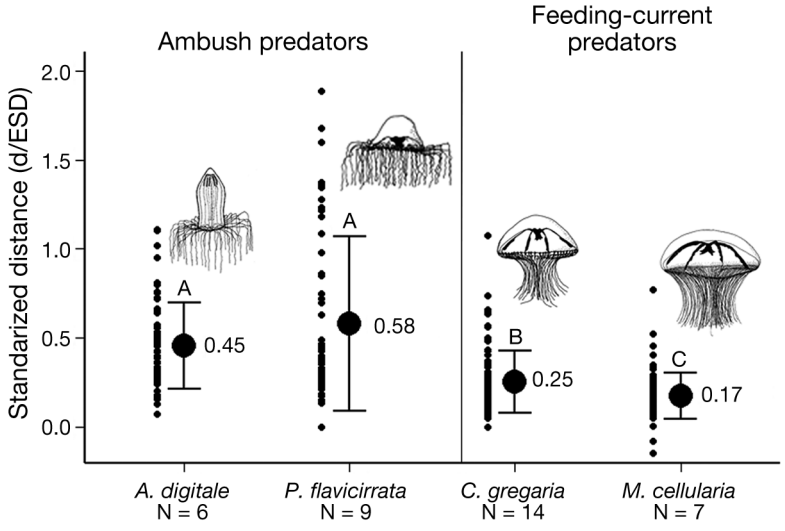

Fig. 1. Distance along tentacle (*d*) normalized to body size (ESD, equivalent spherical diameter) where prey were captured by *Aglantha digitale*, *Proboscidactyla flavicirrata*, *Clytia gregaria* and *Mitrocoma cellularia*. N: number of medusae; large dots: mean distance; error bars: SD. Different letters above error bars: significant differences across rank means (Bonferroni-Dunn test; see Table A1 in the Appendix); small dots: each capture location measurement

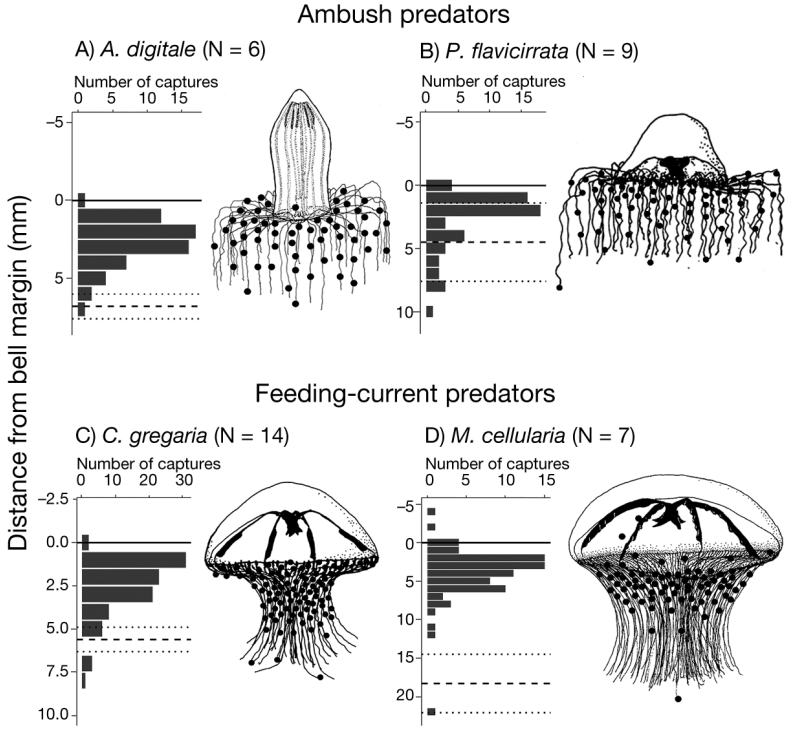

Fig. 2. Cumulative prey capture locations of (A) *Aglantha digitale*, (B) *Proboscidactyla flavicirrata*, (C) *Clytia gregaria* and (D) *Mitrocoma cellularia* feeding on *Artemia* nauplii. N: number of individuals recorded; solid line: bell margin; dashed line: mean tentacle length of the recorded individuals; dotted lines: SD of the mean tentacle length; black dots: all observed capture locations from all individuals (horizontal positions of the dots are arbitrary)

RESULTS

Prey capture locations

Artemia nauplii were captured at different locations relative to the bell margin in the different hydromedusa species (KW χ^2 = 83.18, df = 3, $p < 0.001$; Fig. 1). Captures by the ambush predators *Aglantha digitale* and *Proboscidactyla flavicirrata* occurred further from the bell margin compared to captures by the feeding-current predators *Clytia gregaria* and *Mitrocoma cellularia* (Bonferroni-Dunn, $p < 0.001$; Figs. 1 & 2A,B, Table A1 in the Appendix). Captures in *M. cellularia* were closest to the bell margin compared to the other species (Bonferroni-Dunn, $p < 0.05$ for all comparisons; Table A1). In addition to capture distance, the dispersion of captured prey along the tentacles differed between foraging strategies. Capture locations were more dispersed in the ambush medusae while feeding-current medusae captured most of their prey in a localized region adjacent to the bell (Fig. 2).

Nematocyst density and type across species

The hydromedusae species had different total nematocyst densities (KW χ^2 = 179.77, df = 5, $p < 0.001$; Table 1, Fig. 3, Table A1). The feeding-current predators had higher nematocyst densities compared to the ambush predators. *M. cellularia* had the highest nematocyst densities of all species examined. Table 1 shows weighted means for each nematocyst type. All 3 feeding-current species analyzed had predominantly mastigophore nematocysts. *Aequorea victoria* had a second nematocyst type (isorhizas), however, the mastigophore density was higher than that of isorhizas (KW χ^2 = 103.581, df = 1, $p < 0.001$). In contrast, ambush predator species each had 2 nematocyst types with 4 total types represented. *A. digitale* had similar densities

Table 1. Nematocyst densities (no. per 1000 μm^2) and types in the hydromedusae species analyzed, reported as weighted means (±SD) for individuals with repeated tentacle measurements (n = number of tentacles, N = number of individuals)

Species	Desmo-nemes	Isorhizas	Microbasic euryteles	Mastigo-phores	Stenoteles	Total
Ambush predators						
Aglantha digitale (n = 9, N = 4)	–	–	2.8 ± 1.2	–	2.9 ± 1.9	5.7 ± 2.8
Proboscidactyla flavicirrata (n = 6, N = 5)	2.1 ± 0.8	–	–	2.3 ± 1.0	–	4.4 ± 1.8
Sarsia tubulosa (n = 7, N = 3)	4.9 ± 1.7	–	–	–	1.0 ± 0.5	5.8 ± 2.0
Feeding-current predators						
Aequorea victoria (n = 7, N = 6)	–	0.9 ± 0.4	–	6.1 ± 3.9	–	7.0 ± 4.1
Clytia gregaria (n = 6, N = 5)	–	–	–	11.1 ± 2.1	–	11.1 ± 4.7
Mitrocoma cellularia (n = 5, N = 4)	–	–	–	15.4 ± 2.2	–	15.4 ± 4.3

of microbasic euryteles and stenoteles (KW χ^2 = 0.038, df = 1, p = 0.84). *Proboscidactyla flavicirrata* also had similar densities of desmonemes and mastigophores (KW χ^2 = 0.727, df = 1, p = 0.39), but *Sarsia tubulosa* had 5 times more desmonemes than stenoteles (KW χ^2 = 85.908, df = 1, p < 0.001).

Nematocyst distribution along the tentacles

The distributions of nematocysts on the tentacles were different among the species analyzed. In the ambush predators *P. flavicirrata* and *S. tubulosa*, nematocysts were arranged in clusters (Fig. 4B,C), whereas in the other species nematocysts were dispersed along the tentacles (Fig. 4A,D–F). Nematocyst density increased in a distal direction along the tentacles of the ambush predators *A. digitale*, *P. flavicirrata* and *S. tubulosa* (Fig. 5A–C). *A. victoria* had a uniform nematocyst density throughout the tentacle length (Fig. 5D), and the feeding-current predators *C. gregaria* and *M. cellularia* had higher nematocyst densities in the first half of the tentacle length (Fig. 5E,F).

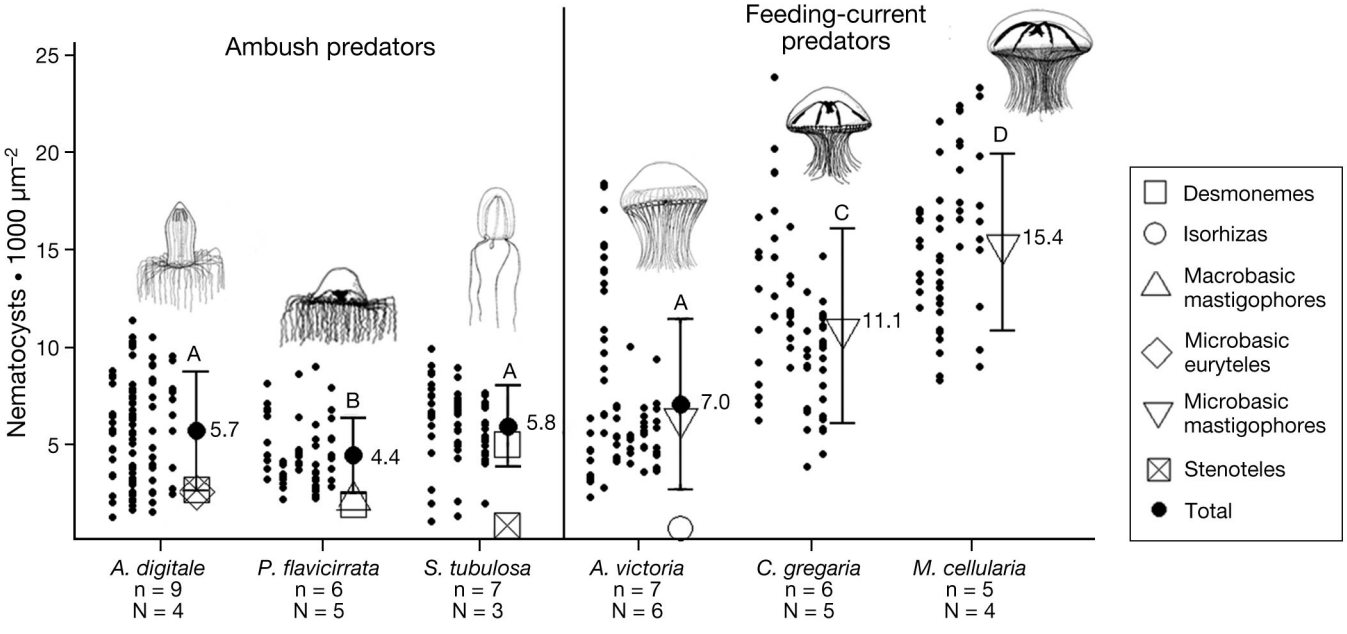

Fig. 3. Nematocyst densities for *Aglantha digitale*, *Proboscidactyla flavicirrata*, *Sarsia tubulosa*, *Aequorea victoria*, *Clytia gregaria* and *Mitrocoma cellularia*. Each small dot represents a single density measurement from one section of the tentacle, grouped in vertical lines for each individual. N: number of hydromedusae per species; n: total number of tentacles analyzed for all individuals of that species. For species with 2 nematocyst types, large dots represent total mean nematocyst density for each species. Error bars: SD (only presented for total nematocysts). Different letters above error bars represent significant differences across rank means (Bonferroni-Dunn test; see Table A1 in the Appendix)

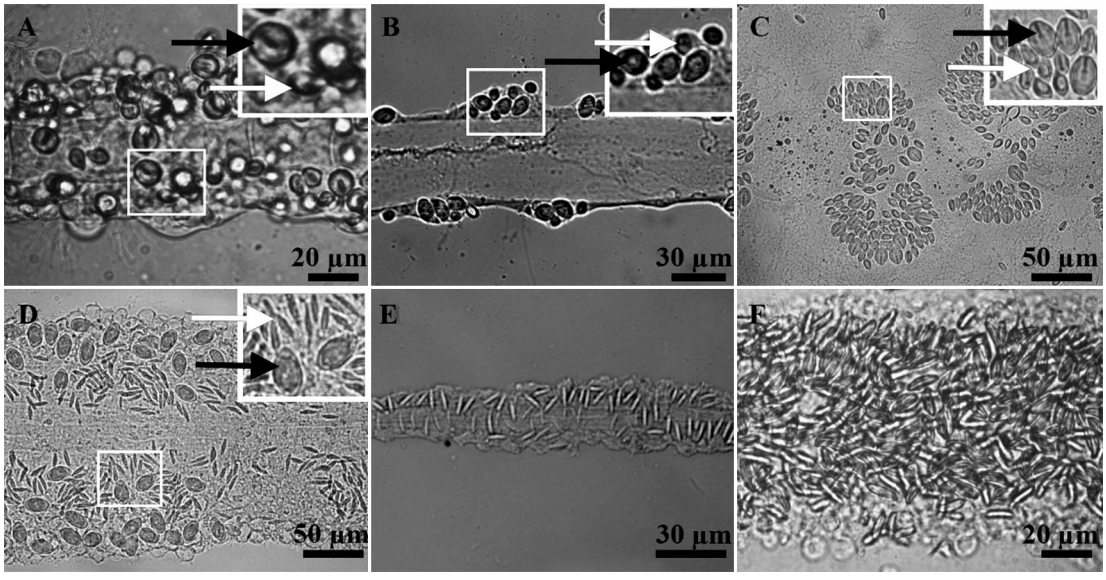

Fig. 4. Nematocysts in the tentacles of (A–C) ambush-feeding and (D–F) current-feeding hydromedusae. White rectangles mark zoomed-in areas, which show different nematocyst types: (A) *Aglantha digitale*: stenoteles (black arrow) and microbasic euryteles (white arrow); (B) *Proboscidactyla flavicirrata*: desmonemes (black arrow) and macrobasic mastigophores (white arrow); (C) *Sarsia tubulosa*: stenoteles (black arrow) and desmonemes (white arrow); (D) *Aequorea victoria*: isorhizas (black arrow) and microbasic mastigophores (white arrow); (E) *Clytia gregaria* and (F) *Mitrocoma cellularia*: microbasic mastigophores only

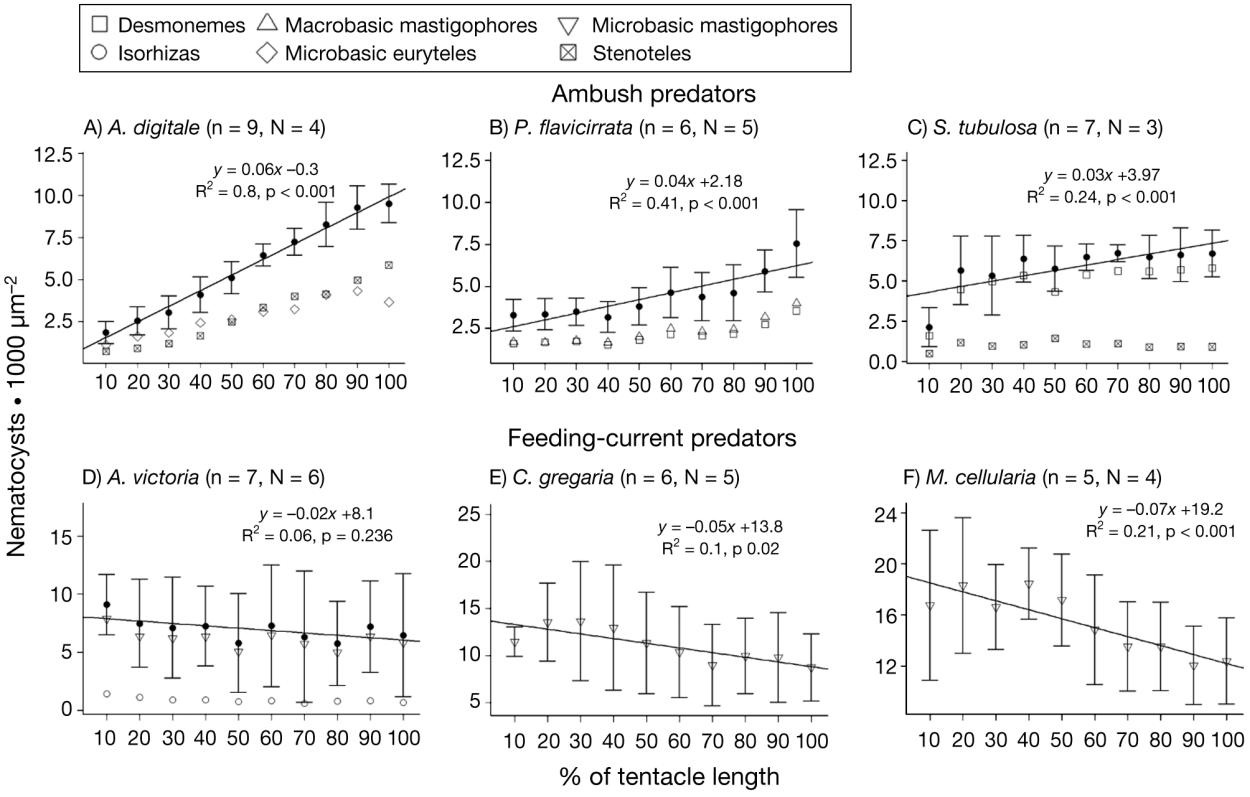

Fig. 5. Nematocyst densities along the tentacle length for (A) *Aglantha digitale*, (B) *Proboscidactyla flavicirrata*, (C) *Sarsia tubulosa*, (D) *Aequorea victoria*, (E) *Clytia gregaria* and (F) *Mitrocoma cellularia*; where 0% is the tentacle base and 100% is the tentacle tip. Black dots for species with >1 nematocyst type represent total nematocyst density. Error bars: SD; n: number of tentacles analyzed; N: number of individuals analyzed. General linear regressions with equation, R^2 values and p-values are shown on each plot only for the total nematocyst abundances

DISCUSSION

Feeding rates and prey selection patterns are determined by the outcome of different stages of the feeding process. The feeding process consists of the encounter, capture and ingestion stages, and prey may escape from the predator at any stage of this process. The encounter process and how it influences feeding rates and prey selection has been well described for ambush and feeding-current medusae (Hansson & Kiørboe 2006, Regula et al. 2009, Katija et al. 2011). However, much less is understood about how the post-encounter stages compare between ambush and feeding-current medusae. It has been shown, however, that post-encounter success is critical for determining the predatory impact of gelatinous predators (Colin et al. 2015). Our feeding observations revealed that prey were not captured uniformly along prey capture surfaces, and that capture locations related directly to foraging mode. Ambush predator medusae captured more prey further from the bell compared to feeding-current medusae (Fig. 2). In addition, the density, distribution and type of nematocysts related to foraging mode. Consistent with prey captures, ambush-feeding medusae had higher nematocyst counts toward the tentacle tips (Fig. 5A–C). In contrast, the nematocysts of the feeding-current predators were either distributed evenly along the tentacle length or were denser near the bell margin (Fig. 5D–F). Furthermore, relative numbers of nematocysts of different types varied among species (Table 1). These results help explain the different prey capture patterns of the hydromedusae.

Comparative prey capture locations

The prey encounter volume of a hydromedusa is based on the tentacle number and positioning of the tentacles around the bell (Madin 1988). However, capture within this encounter volume is also affected by each species' behavior (Madin 1988, Ford et al. 1997, Colin et al. 2005). For instance, oblate medusa with disc-shaped umbrellas are considered feeding-current predators; with each bell contraction and relaxation they create starting and stopping vortices, respectively, that circulate fluid through the tentacles (Colin & Costello 2002, Dabiri et al. 2006, Katija et al. 2011). The starting vortex entrains fluid adjacent to the bell and transports it through the tentacles near the bell margin then downstream from the bell (Dabiri et al. 2006, Katija et al. 2011). Transport of fluid through the tentacles continues during bell expansion as the stopping vortex entrains and transports more fluid through the tentacles near the bell and up into the subumbrellar cavity (Dabiri et al. 2006, Katija et al. 2011). Consequently, flow during both phases of the swimming cycle moves fluid through the tentacles near the bell and results in captures close to the bell margin (Fig. 2C,D, Ford et al. 1997). Understanding how prey are transported during this process in conjunction with nematocyst and capture locations reveals that capture surfaces near the bell appear to be most important in the feeding process for feeding-current medusae. For example, we saw that for both *Clytia gregaria* and *Mitrocoma cellularia*, the combination of flow and morphology resulted in most captures occurring adjacent to the bell margin, with number of captures and nematocyst densities declining with distance from the bell.

Captures by ambush-feeding medusae were more randomly distributed (Figs. 1 & 2A–B). Most gelatinous ambush predators feed by remaining stationary in the water column with their tentacles extended (Colin et al. 2003); capture occurs when prey collide with the tentacles (Gerritsen & Strickler 1977, Purcell 1981, Greene 1985, Costello 1992). The distance between adjacent tentacles increases further from the bell margin (Madin 1988). This would serve to lower encounter rates with prey with distance from the bell. However, nematocyst densities increase with distance from the bell and this should increase capture efficiencies, which may compensate for decreased encounter rates. Thus, it is likely that the combined effects of morphology on encounters (i.e. tentacle array) and captures (i.e. nematocyst distribution) result in capture locations occurring more uniformly along the length of the tentacles of ambushing medusa.

Spatial nematocyst distribution in the tentacles and prey capture

Tentacle traits such as high nematocyst densities at capture locations in medusae will likely increase capture efficiency (Regula et al. 2009). Several studies have documented increased nematocyst densities in the regions of the medusan body where prey are captured. For instance, in *Cyanea capillata* the relative importance of different anatomical structures used in prey capture can change during ontogeny due to mechanical constraints, and nematocyst density is higher where prey captures are more frequent (Higgins et al. 2008). The small leptomedusa, *Obelia* sp., only overcomes viscous boundary layers at the tentacle tips during rapid contractions, allowing for prey cap-

ture at these surfaces; correspondingly, nematocyst numbers are highest at the tentacle tips (Sutherland et al. 2016). 'Tentacle first' swimming behavior in cruising medusae such as *Solmissus incisa* maximizes stealthy prey capture (Raskoff 2002); nematocysts are located only on the upper side of *Solmissus* tentacles, which has been interpreted as an indication of prey capture location (Mills & Goy 1988).

Decreasing, increasing or constant nematocyst density toward the tentacle tips such as the ones described here for ambush and feeding-current hydromedusae species (Fig. 5) could have a significant effect on the transfer efficiencies of variable prey types, since capture locations are different for each species (Fig. 2) and adherence force between the prey and the capture surface of a predator is determined in part by the number of nematocyst fired in each encounter (Thorington & Hessinger 1996).

Differential nematocyst density, type and prey selectivity

Prey selectivity is affected by the number and type of nematocysts discharged during each prey capture event but there may not be a straightforward relationship between number of nematocysts and prey size. For instance, siphonophores that feed on large prey tend to have fewer nematocyst batteries per tentacle (Purcell 1984). We found that ambush predators, which feed on relatively large prey, had low nematocyst densities compared to the feeding-current hydromedusae that eat small prey (Table 1, Fig. 3). Ambush-feeding *Aglantha digitale* and *Sarsia tubulosa* ingest copepodites and adult copepods (Purcell & Mills 1988, Colin & Costello 2002) and *Proboscidactyla flavicirrata* primarily consumes veliger larvae (Purcell & Mills 1988, Colin & Costello 2002). The feeding-current medusae *C. gregaria* and *M. cellularia* had the highest nematocyst densities of all species analyzed (Table 1); both species prefer smaller prey items such as invertebrate eggs (Purcell & Mills 1988, Colin & Costello 2002).

Prey selectivity also relates to the predator's nematocyst type. Desmonemes usually adhere to the surface of hard-bodied prey, isorhizas penetrate soft-bodied prey and mastigophores and stenoteles can either adhere to or penetrate prey (Purcell & Mills 1988). It has been noted that ambush-feeding medusae consume hard-bodied prey and usually have 2 types of nematocysts; in contrast, feeding-current medusae that feed upon soft-bodied prey have a predominant nematocyst type, which are usually mastigophores (Purcell & Mills 1988). We found that the ratios of different nematocysts can also vary. *S. tubulosa* had 5 times more desmonemes than stenoteles, whereas the other ambush-feeding species had similar densities for both nematocyst types. *Aequorea victoria* also had an imbalanced proportion of 2 nematocyst types, with 6 times more microbasic mastigophores than isorhizas (Table 1, Fig. 3). Since adherence force between tentacle and prey can change according to the number and the kind of discharging cnidae (Thorington & Hessinger 1996), it is likely that differential densities of each nematocyst type would produce variable adherence force between the prey and the tentacle surface, which would either prevent or facilitate attachment to the tentacles.

CONCLUSIONS

Understanding how morphological traits mediate predator–prey interactions allows us to predict how a given predator might affect the community composition of lower trophic levels. This might be especially relevant for changing marine ecosystems where planktonic predators such as medusae can become highly abundant due to accelerated reproductive rates (Purcell 2005). Despite an increasing recognition that gelatinous predators help structure food webs, small hydromedusae (<1 cm) remain understudied even though they represent most of medusan diversity (>60%; Colin et al. 2005). The relationships among functional morphology and dietary niches of coexisting hydromedusae are key for understanding the ordering principles that determine trophic patterns in these organisms (Costello & Colin 2002). Here, we demonstrated that the interaction between morphological and behavioral traits determines prey capture locations. Furthermore, locations of prey capture and nematocyst distribution in the tentacles change according to guild associations of hydromedusae. Differences among these traits might also be related to the distinct prey selectivity patterns within species with similar feeding modes. This trait-based understanding of the functional roles of marine predators will be useful for incorporating the predatory impact of less-studied gelatinous predators into food web models.

Acknowledgements. We thank Richard Emlet for providing useful advice and John Costello and Brad Gemmell for helping define the experimental setup. This project was supported by the Patricia L. Dudley endowment (M.C.U.) and the National Science Foundation (OCE-1155084 to KRS, OCE- 1536688 to SPC) and Oregon Sea Grant (K.R.S.).

LITERATURE CITED

Brooks JL, Dodson SI (1965) Predation, body size and composition of plankton. Science 150:28–35

Bouillon J (1985) Notes additionelles sur les Hydroméduses de la mer de Bismarck (Hydrozoa-Cnidaria). Indo-Malayan Zool. 2:245–266

Colin SP, Costello JH (2002) Morphology, swimming performance and propulsive mode of six co-occurring hydromedusae. J Exp Biol 205:427–437

Colin SP, Costello JH, Klos E (2003) *In situ* swimming and feeding behavior of eight co-occurring hydromedusae. Mar Ecol Prog Ser 253:305–309

Colin SP, Costello JH, Graham W, Higgins J III (2005) Omnivory by the small cosmopolitan hydromedusa *Aglaura hemistoma.* Limnol Oceanogr 50:1264–1268

Colin SP, MacPherson R, Gemmell B, Costello JH, Sutherland K, Jaspers C (2015) Elevating the predatory effect: sensory-scanning foraging strategy by the lobate ctenophore *Mnemiopsis leidyi.* Limnol Oceanogr 60:100–109

Costello J (1992) Foraging mode and energetics of hydrozoan medusae. Sci Mar 53:185–191

Costello JH, Colin SP (1994) Morphology, fluid motion and predation by the scyphomedusa *Aurelia aurita.* Mar Biol 121:327–334

Costello JH, Colin SP (1995) Flow and feeding by swimming scyphomedusae. Mar Biol 124:399–406

Costello JH, Colin SP (2002) Prey resource use by coexisting hydromedusae from Friday Harbor, Washington. Limnol Oceanogr 47:934–942

Costello JH, Colin SP, Dabiri JO (2008) Medusan morphospace: phylogenetic constraints, biomechanical solutions, and ecological consequences. Invertebr Biol 127: 265–290

Dabiri JO, Colin SP, Costello JH (2006) Fast-swimming hydromedusae exploit velar kinematics to form an optimal vortex wake. J Exp Biol 209:2025–2033

Dabiri JO, Colin SP, Katija K, Costello JH (2010) A wake-based correlate of swimming performance and foraging behavior in seven co-occurring jellyfish species. J Exp Biol 213:1217–1225

Denker E, Manuel M, Leclére L, Le Guyader H, Rabert N (2008) Ordered progression of nematogenesis from stem cells through differentiation stages in the tentacle bulb of *Clytia hemisphaerica* (Hydrozoa, Cnidaria). Dev Biol 315:99–113

Dinno A (2016) dunn.test: Dunn's test of multiple comparisons using rank sums. R package version 1.3.2. http://CRAN.R-project.org/package=dunn.test

Dunn OJ (1961) Multiple comparisons among means. J Am Stat Assoc 56:52–64

Fields DM, Yen J (1997) The escape behavior of marine copepods in response to a quantifiable fluid mechanical disturbance. J Plankton Res 19:1289–1304

Ford MD, Costello JH, Heidelberg KB, Purcell JE (1997) Swimming and feeding by the scyphomedusa *Chrysaora quinquecirrha.* Mar Biol 129:355–362

Gemmell BJ, Troolin DR, Costello JH, Colin SP, Satterlie RA (2015) Control of vortex rings for manoeuvrability. J R Soc Interface 12:20150389

Gerritsen J, Strickler JR (1977) Encounter probabilities and community structure in zooplankton: a mathematical model. J Fish Res Board Can 34:73–82

Greene CH (1985) Planktivore functional groups and patterns of prey selection in pelagic communities. J Plankton Res 7:35–40

Greene CH (1988) Foraging tactics and prey-selection patterns of omnivorous and carnivorous copepods. Hydrobiologia 167-168:295–302

Hansson LJ, Kiørboe T (2006) Prey-specific encounter rates and handling efficiencies as causes of prey selectivity in ambush-feeding hydromedusae. Limnol Oceanogr 51: 1849–1858

Higgins JE III, Ford MD, Costello JH (2008) Transitions in morphology, nematocyst distribution, fluid motions, and prey capture during development of the scyphomedusa *Cyanea capillata.* Biol Bull (Woods Hole) 214: 29–41

Hirst AG, Roff JC, Lampitt RS (2003) A synthesis of growth rates in marine epipelagic invertebrate zooplankton. Adv Mar Biol 44:1–142

Katija K, Beaulieu WT, Regula C, Colin SP, Costello JH, Dabiri JO (2011) Quantification of flows generated by the hydromedusa *Aequorea victoria*: a Lagrangian coherent structure analysis. Mar Ecol Prog Ser 435:111–123

Larson RJ (1987) Trophic ecology of planktonic gelatinous predators in Saanich Inlet, British Columbia: diets and prey selection. J Plankton Res 9:811–820

Madin L (1988) Feeding behaviour of tentaculate predators: in situ observations and a conceptual model. Bull Mar Sci 43:413–429

Mills C (1981) Diversity of swimming behaviors in hydromedusae as related to feeding and utilization of space. Mar Biol 64:185–189

Mills C, Goy J (1988) In situ observations of the behavior of mesopelagic *Solmissus* Narcomedusae (Cnidaria, Hydrozoa). Bull Mar Sci 43:739–751

Östman C (2000) A guideline to nematocyst nomenclature and classification, and some notes on the systematic value of nematocysts. Sci Mar 64:31–46

Pitt KA, Duarte CM, Lucas CH, Sutherland KR and others (2013) Jellyfish body plans provide allometric advantages beyond low carbon content. PLoS ONE 8: e72683

Purcell JE (1981) Selective predation and caloric consumption by the siphonophore *Rosacea cymbiformis* in nature. Mar Biol 63:283–294

Purcell JE (1984) The functions of nematocyst in prey capture by epipelagic siphonophores. Biol Bull (Woods Hole) 166:310–327

Purcell JE (1997) Pelagic cnidarians and ctenophores as predators: selective predation, feeding rates, and effects on prey populations. Ann Inst Oceanogr Paris (Nouv Ser) 73:125–137

Purcell JE (2005) Climate effects on formation of jellyfish and ctenophore blooms: a review. J Mar Biol Assoc UK 85:461–473

Purcell JE, Grover JJ (1990) Predation and food limitation as causes of mortality in larval herring at a spawning ground in British Columbia. Mar Ecol Prog Ser 59: 55–61

Purcell JE, Mills CE (1988) The correlation between nematocyst types and diets in pelagic hydrozoa. In: Hessinger DA, Lenoff HM (eds) The biology of nematocysts. Academic Press, San Diego, CA, p 463–485

Purcell JE, Silferd TD, Marliave JB (1987) Vulnerability of larval herring (*Clupea harengus pallasi*) to capture by the jellyfish *Aequorea victoria.* Mar Biol 94:157–162

Raskoff K (2002) Foraging, prey capture and gut contents of

the mesopelagic narcomedusa *Solmissus* spp. (Cnidaria: Hydrozoa). Mar Biol 141:1099–1107

Regula C, Colin SP, Costello JH, Kordula H (2009) Prey selection mechanism of ambush-foraging hydromedusae. Mar Ecol Prog Ser 374:135–144

Richardson AJ (2008) In hot water: zooplankton and climate change. ICES J Mar Sci 65:279–295

Sutherland KR, Gemmell BJ, Colin SP, Costello JH (2016) Prey capture by the cosmopolitan hydromedusa, *Obelia* spp., in the viscous regime. Limnol Oceanogr 61: 2309–2317

Thorington GU, Hessinger DA (1996) Efferent mechanisms of discharging cnidae: I. Measurements of intrinsic adherence of cnidae discharged from tentacles of the sea anemone, *Aiptasia pallida*. Biol Bull (Woods Hole) 190: 125–138

Appendix

Table A1. Bonferroni-Dunn comparisons between species of hydromedusae. Aeq: *Aequorea*; Agl: *Aglantha*; Cly: *Clytia*; Mit: *Mitrocoma*; Pro: *Proboscidactyla*; Sar: *Sarsia*. Values in **bold** represent significance at $p < 0.05$

Variable	Species pair	Dunn's *z*	Probability
Relative capture distance	Cly–Agl	5.49	**<0.0001**
	Mit–Agl	7.61	**<0.0001**
	Mit–Cly	2.62	**0.0257**
	Pro–Agl	0.50	1.0000
	Pro–Cly	−4.88	**<0.0001**
	Pro–Mit	−7.00	**<0.0001**
Nematocyst density	Agl–Aeq	1.10	1.0000
	Cly–Aeq	−5.36	**<0.0001**
	Cly–Agl	−6.71	**<0.0001**
	Mit–Aeq	−8.09	**<0.0001**
	Mit–Agl	−9.48	**<0.0001**
	Mit–Cly	−2.89	**0.0287**
	Pro–Aeq	3.60	**0.0024**
	Pro–Agl	2.75	**0.0444**
	Pro–Cly	8.64	**<0.0001**
	Pro–Mit	11.13	**<0.0001**
	Sar–Aeq	0.45	1.0000
	Sar–Agl	−0.62	1.0000
	Sar–Cly	5.80	**<0.0001**
	Sar–Mit	8.50	**<0.0001**
	Sar–Pro	−3.17	**0.0114**

Editorial responsibility: Sigrun Jónasdóttir, Charlottenlund, Denmark

Submitted: August 1, 2016; Accepted: January 16, 2017
Proofs received from author(s): March 16, 2017